**Cell Reports Methods, Volume *2***

## Supplemental information

# A culture platform to study quiescent hematopoietic stem cells following genome editing

**Kohei Shiroshita, Hiroshi Kobayashi, Shintaro Watanuki, Daiki Karigane, Yuriko Sorimachi, Shinya Fujita, Shinpei Tamaki, Miho Haraguchi, Naoki Itokawa, Kazumasa Aoyoama, Shuhei Koide, Yosuke Masamoto, Kenta Kobayashi, Ayako Nakamura-Ishizu, Mineo Kurokawa, Atsushi Iwama, Shinichiro Okamoto, Keisuke Kataoka, and Keiyo Takubo**

## SUPPLEMENTAL FIGURES AND LEGENDS

# Figure S1

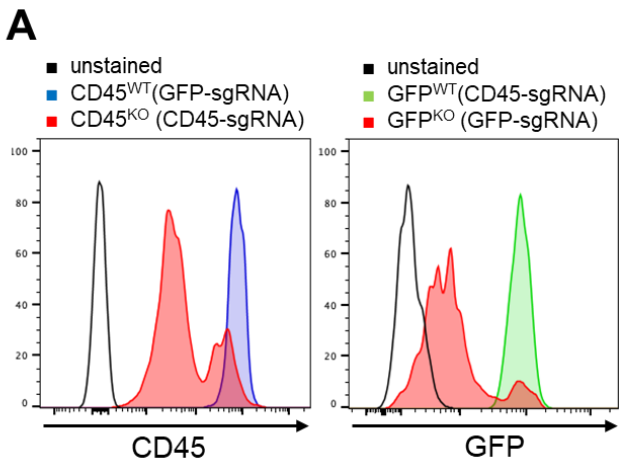


B

| | CD45 | GFP |
|---|---|---|
| homo | 60.8(%) | 86.4(%) |
| hetero | 17.6(%) | 2.3%(%) |
| WT | 21.6(%) | 11.3(%) |

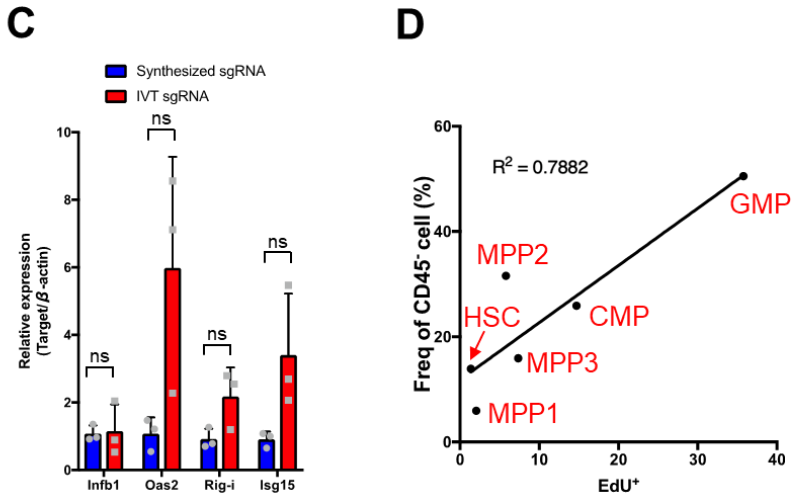


**Figure S1. The cell cycle status determines the genome editing efficiency of HSPC fractions, related to Figure 1**

(A) A representative flow cytometry histogram of CD45 and GFP expression levels in edited HSCs from Ubc-GFP homozygous mice. The genome editing efficiency was determined at 3 days after electroporation.

(B) Table of genotyping results after analysis of gene editing in single colonies. Genome-edited HSCs were electroporated with CD45-sgRNA or GFP-sgRNA and cultured in Methocult M3434. A single colony was picked and Sanger sequencing was performed. The sequencing results were analyzed by TIDE (n = 51 and 44 colonies for the CD45-edited and GFP-edited groups, respectively).

(C) qPCR analysis comparing expression of IFN signaling-related genes upon treatment with IVT and synthesized sgRNAs (mean ± SD, n = 3 from three independent electroporation). The two-tailed Student's t test was used.

(D) Correlation between the frequency of cells in S phase and the genome editing efficiency among HSPC fractions.

# Figure S2

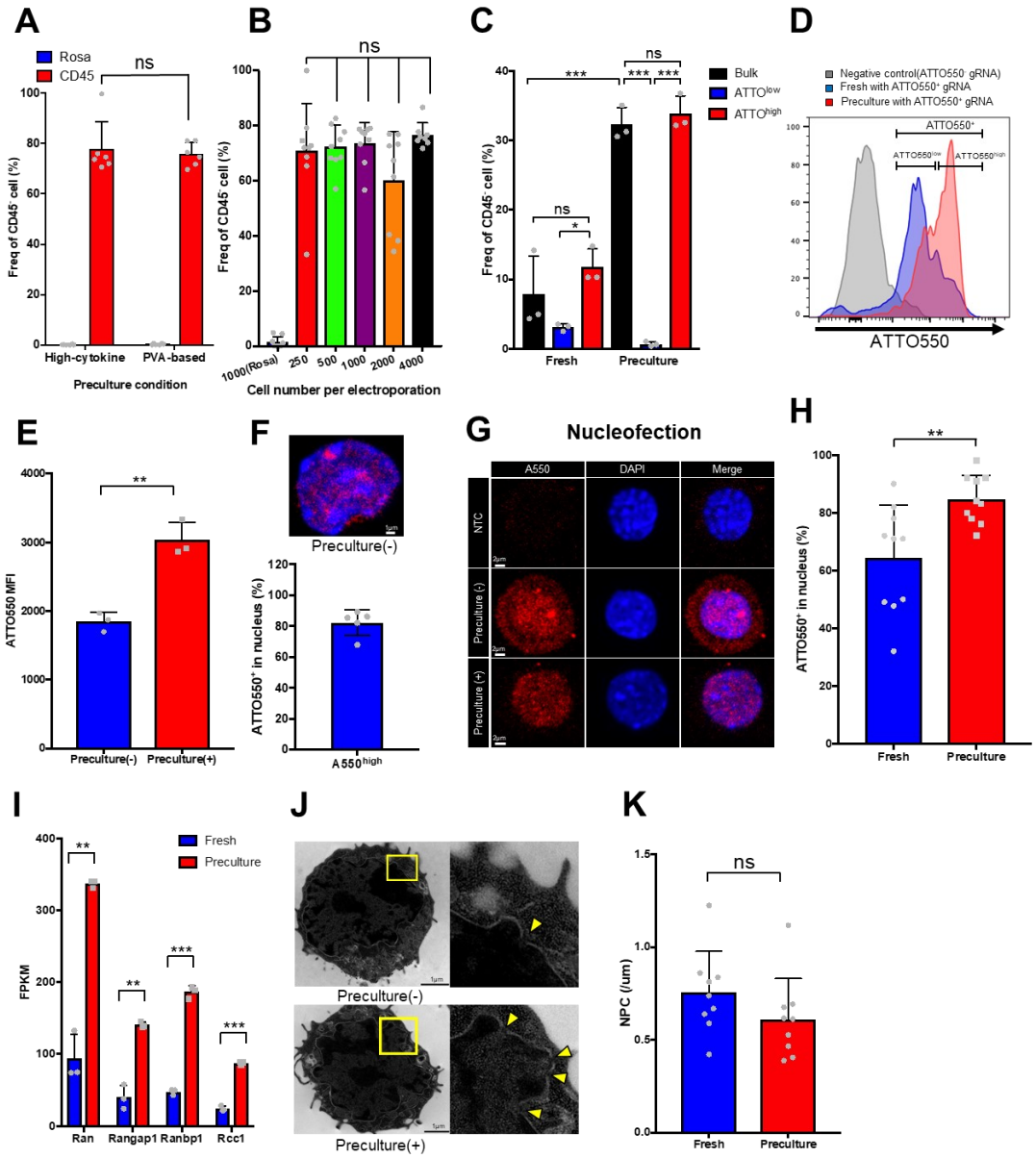


**Figure S2. The preculture, but not the post-culture, condition defines the genome editing efficiency of HSCs, related to Figure 2**

(A) Comparison of the genome editing efficiency of LSK cells between the high cytokine and PVA-based conditions (mean ± SD, n = 6 per group from two independent experiments). The two-tailed Student's t test was used.

(B) Genome editing efficiency according to the number of HSCs per experiment (mean ± SD, n = 8–9 per group from four independent experiments). The Tukey-Kramer multiple comparisons test was used.

(C) Validation of the editing outcome using ATTO550-labeled gRNA in fresh and precultured LSK cells (mean ± SD, n = 3 per group from four independent experiments). The Tukey-Kramer multiple comparisons test was used.

(D) Representative histogram of fresh (blue) and precultured (red) LSK cells immediately after electroporation of ATTO550-labeled gRNA (mean ± SD, n = 3 per group from four independent electroporations). Non-labeled gRNA was used as a negative control (gray).

(E) Mean fluorescence intensity of ATTO550 in fresh (blue) and precultured (red) LSK cells was analyzed immediately after electroporation of ATTO550-labeled gRNA (n = 3 per group from three independent electroporations). The two-tailed Student's t test was used.

(F) Nuclear co-localization levels in ATTO550$^{high}$ LSK cells without preculture. A representative confocal image (upper) and the frequency of nuclear co-localization (lower) (mean ± SD, n = 5) are shown.

(G) Confocal imaging of freshly isolated and precultured LSK cells immediately after nucleofection with ATTO550-labeled RNP. Nuclei were stained with 4′,6-diamidino-2-phenylindole (DAPI). Non-labeled RNP was used as a negative control (NTC). Representative images are shown.

(H) Frequency of nuclei containing ATTO550-labeled RNP after nucleofection (n = 10 cells/group). The two-tailed Student's t test was used.

(I) FPKM of nuclear import shuttle-related genes in fresh and precultured HSCs determined by RNA-seq analysis (n = 3 per group from three independent experiments). The two-tailed Student's t test was used.

(J) Representative transmission electron microscopy of fresh (upper panel) and precultured (lower panel) electroporated LSK cells. Right panels show high magnifications of the boxed areas in the left panels. Arrowheads depict nuclear pores.

(K) Number of nuclear pores per circumference of the nuclear membrane (n = 9 per group). The two-tailed Student's t test was used.

# Figure S3

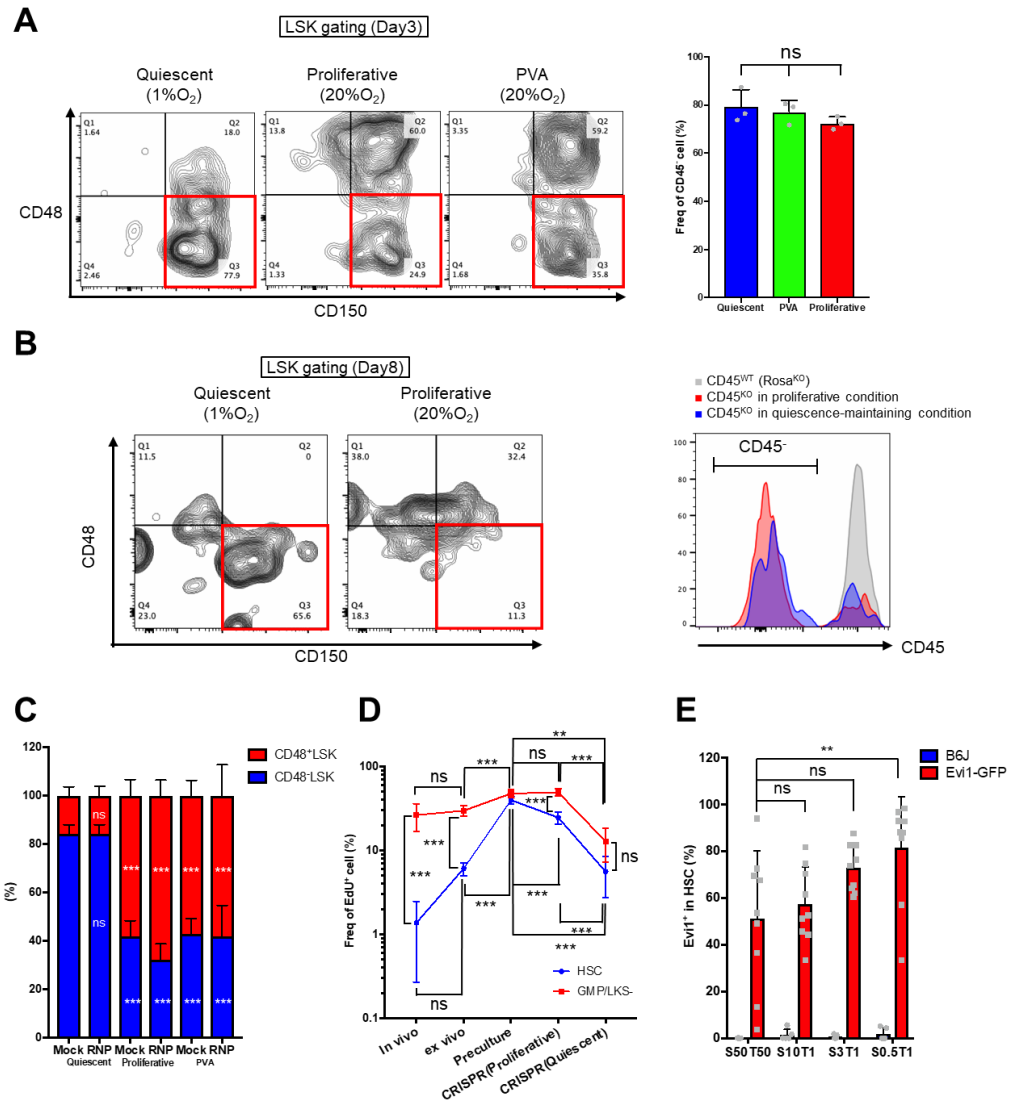


**Figure S3. Post-culture reverts edited HSCs to quiescence, related to Figure 3**

(A) Representative flow cytometry plots of HSCs cultured under the quiescence-maintaining condition (left panel), proliferative condition (middle panel), and PVA-based medium (right panel) at 2 days after electroporation. The frequency of $CD45^-$ cells is shown in the right figure at 2 days after electroporation (mean ± SD, n = 3 per group from three independent cell cultures).

(B) Representative flow cytometry plots of HSCs cultured under the quiescence-maintaining condition (left panel) and proliferative condition (middle panel). The frequency of $CD45^-$ cells is shown in the histogram (right panel) at 7 days after electroporation.

(C) Frequencies of $CD48^+$ and $CD48^-$ LSK cells at 2 days after culture under the quiescence-maintaining, proliferative, and PVA-based conditions (mean ± SD, n = 3 per group from independent cell cultures).

(D) Cell cycle kinetics of edited HSCs evaluated by the EdU incorporation assay. Fresh means *in vivo* EdU labeling, while the other groups were labeled with EdU *in vitro*. The Tukey-Kramer multiple comparisons test was used.

(E) Frequency of $Evi1^+CD150^+CD48^-$ LSK cells cultured under the indicated cytokine conditions in 1% $O_2$ (mean ± SD, n = 9 per group from three independent experiments). The Tukey-Kramer multiple comparisons test was used.

# Figure S4

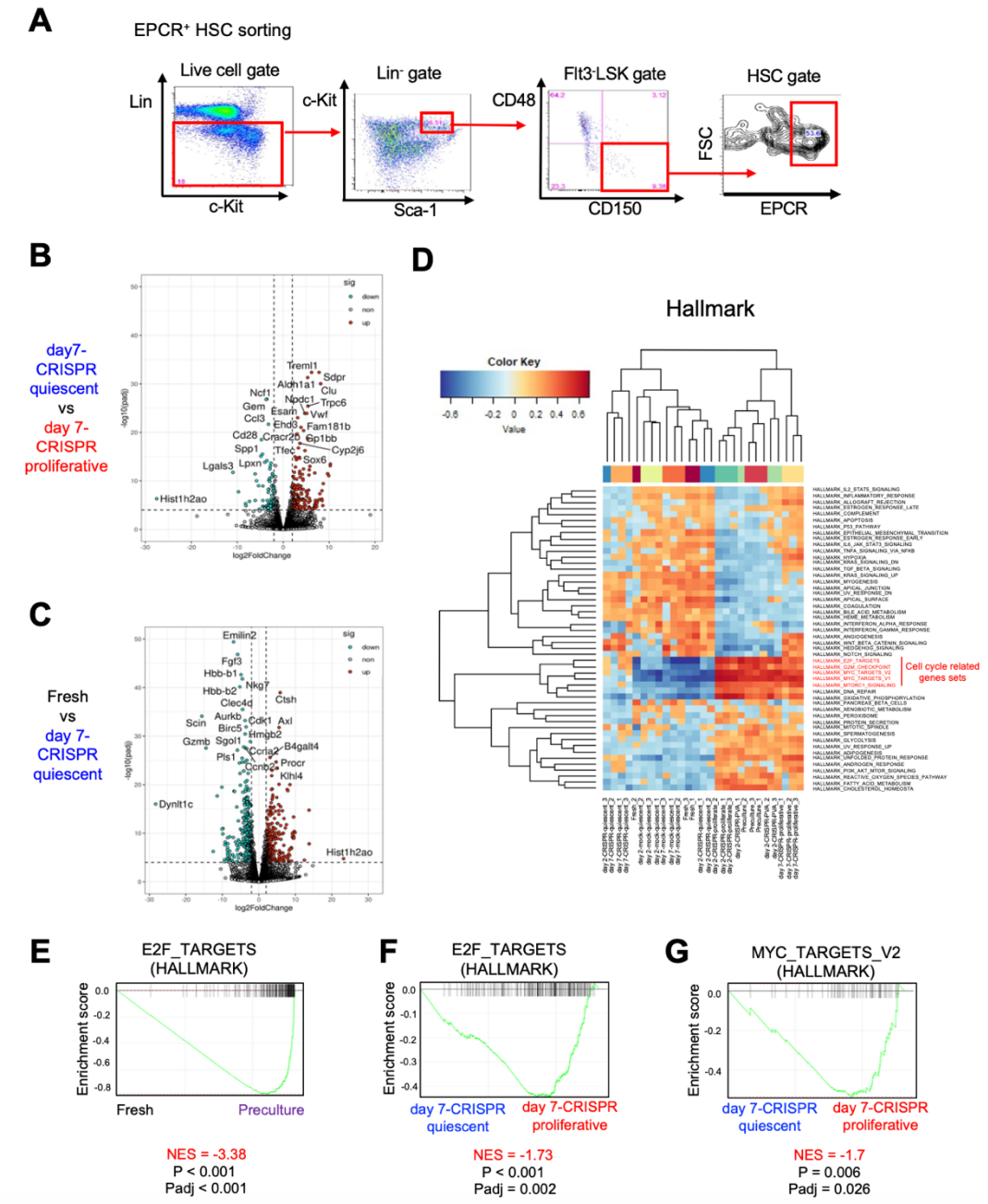


**Figure S4. Sorting strategy for RNA-seq, related to Figure 4**

(A) Representative flow cytometry plot for sorting RNA-seq samples shown in Figure 4A.

(B) Volcano plots comparing the expression levels of various genes between day 7-CRISPR-quiescent and day 7-CRISPR-proliferative.

(C) Volcano plots comparing the expression levels of various genes between fresh and day 7-CRISPR-quiescent.

(D) Hierarchical clustering of single sample GSEA of Hallmark sets by GSVA.

(E) GSEA of E2F target genes comparing fresh and preculture.

(F) GSEA of E2F target genes comparing day 7-CRISPR-quiescent and day 7-CRISPR-proliferative.

(G) GSEA of Myc target genes comparing day 7-CRISPR-quiescent and day 7-CRISPR-proliferative.

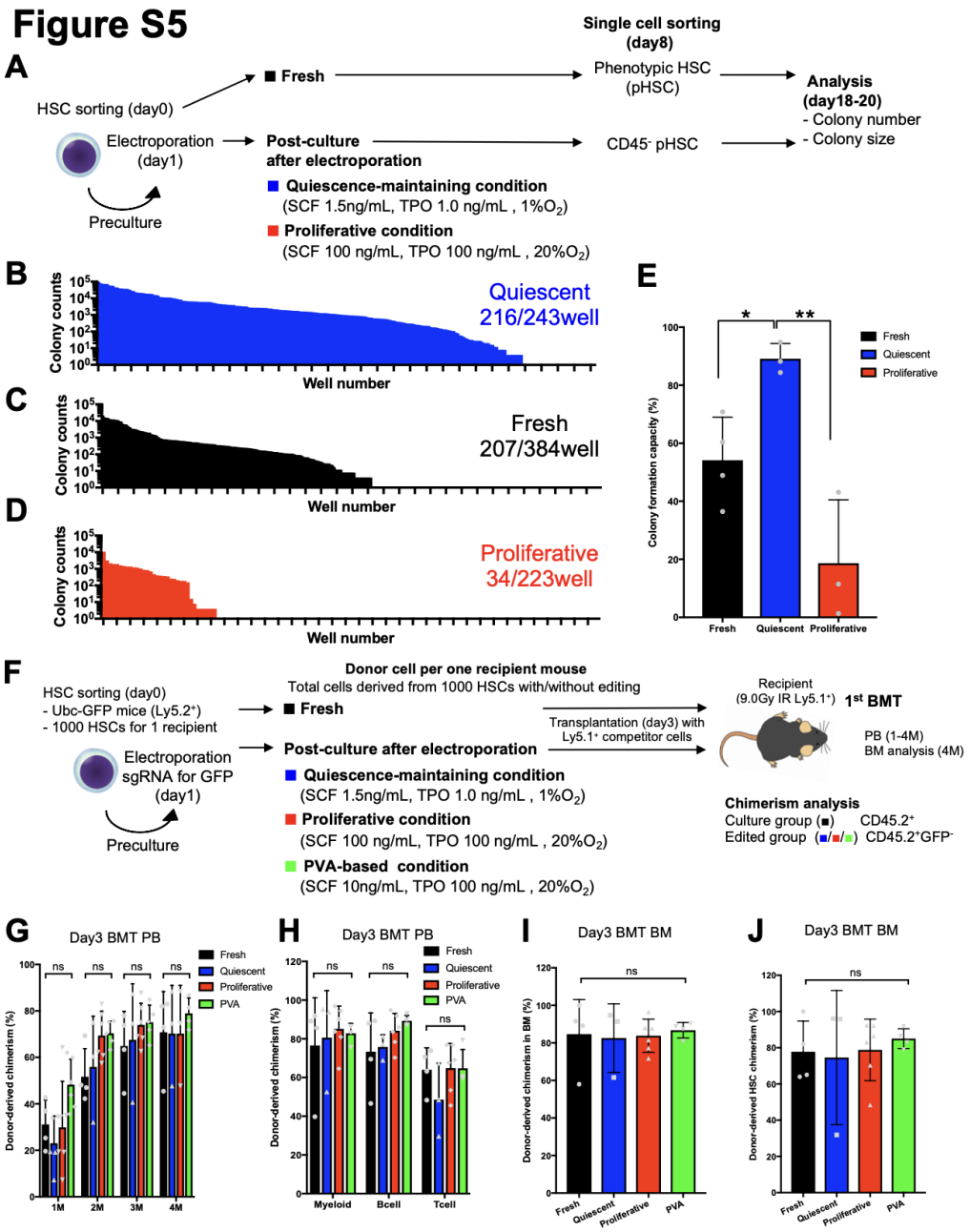


**Figure S5. Colony formation assay of fresh and edited HSCs, related to Figure 5**

(A) Experimental design for the single-cell colony formation assay.

(B–D) Colony forming capacity and cell number of single colonies derived from CD45$^-$ HSCs cultured under the quiescence-maintaining condition (B), fresh HSCs (C), and CD45$^-$ HSCs cultured under the proliferative condition (D) (n = 243, 384, and 223 wells, respectively, from 3–4 independent experiments).

(E) Summary of the colony forming assay results in (B–D) (mean ± SD, n = 3–4 per group from 3–4 independent experiments). The Tukey-Kramer multiple comparisons test was used.

(F) Experimental design of the day 3 transplantation assay of fresh and genome-edited HSCs. Edited HSCs were cultured for 2 days after electroporation, with medium changed daily. Edited HSCs were cultured under quiescence-maintaining conditions (1.5 ng/mL SCF and 1 ng/mL TPO), proliferative conditions (100 ng/mL SCF and 100 ng/mL TPO), and PVA-based conditions (10 ng/mL SCF and 100 ng/mL TPO). Donor cells were transplanted with 0.5 × $10^6$ Ly5.1$^+$ competitor cells.

(G) Peripheral blood chimerism of donor-derived cells following primary transplantation of day 3 (mean ± SD, n =

3–6). The Tukey-Kramer multiple comparisons test was used.

(H) Peripheral blood chimerism of donor-derived myeloid cells, B cells, and T cells following primary transplantation of day 3 (mean ± SD, n = 3–6). The Tukey-Kramer multiple comparisons test was used.

(I) BM chimerism of donor-derived cells following primary transplantation of day 3 (mean ± SD, n = 3–6). The Tukey-Kramer multiple comparisons test was used.

(J) Donor-derived HSC chimerism following primary transplantation of day 3 (mean ± SD, n = 3–6). The Tukey-Kramer multiple comparisons test was used.

# Figure S6

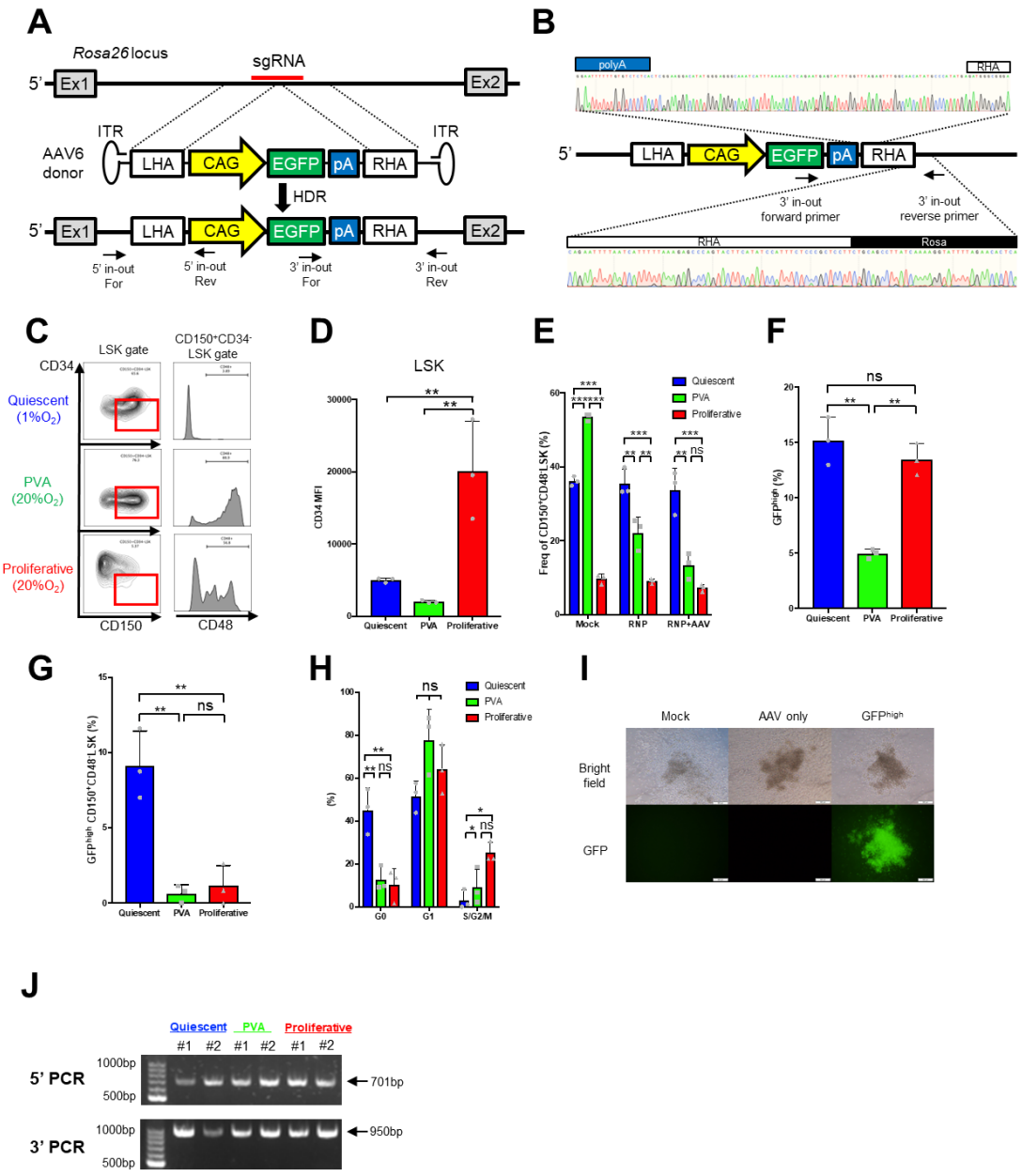


**Figure S6. Quiescent culture is beneficial for HDR-based editing, related to Figure 6**

(A) Targeting strategy to insert EGFP under the control of the CAG promoter into the *Rosa26* locus.

(B) Sanger sequencing of GFP$^{high}$ LSK cells.

(C) Representative flow cytometry plots of edited HSCs at 2 days after AAV6 transduction under the quiescence-maintaining condition (upper panel), PVA-based condition (middle panel), and proliferative condition (lower panel). The right panels showed histograms of CD48 expression under each culture condition.

(D) MFI of CD34 in edited HSCs at 2 days after AAV6 transduction (mean ± SD, n = 3 per group from independent cell cultures). The Tukey-Kramer multiple comparisons test was used.

(E) Frequency of CD150$^{+}$CD48$^{-}$ LSK cells at 2 days after AAV6 transduction (mean ± SD, n = 3 from independent cell cultures). The Tukey-Kramer multiple comparisons test was used.

(F) Frequency of GFP$^{high}$ cells at 2 days after AAV6 transduction (mean ± SD, n = 3 from independent cell cultures). The Tukey-Kramer multiple comparisons test was used.

(G) Frequency of GFP$^{high}$ CD150$^{+}$CD48$^{-}$ LSK cells at 2 days after AAV6 transduction (mean ± SD, n = 3 from

independent cell cultures). The Tukey-Kramer multiple comparisons test was used.

(H) Cell cycle status at 2 days after AAV6 transduction (mean ± SD, n = 3 from independent cell cultures). The Tukey-Kramer multiple comparisons test was used.

(I) Representative images of colonies and EGFP expression.

(J) Representative agarose gel for the specific 5’ and 3’ PCRs performed using individually picked CFUs from cells edited with the AAV-GFP donor (n = 2 per culture condition).

## Figure S7

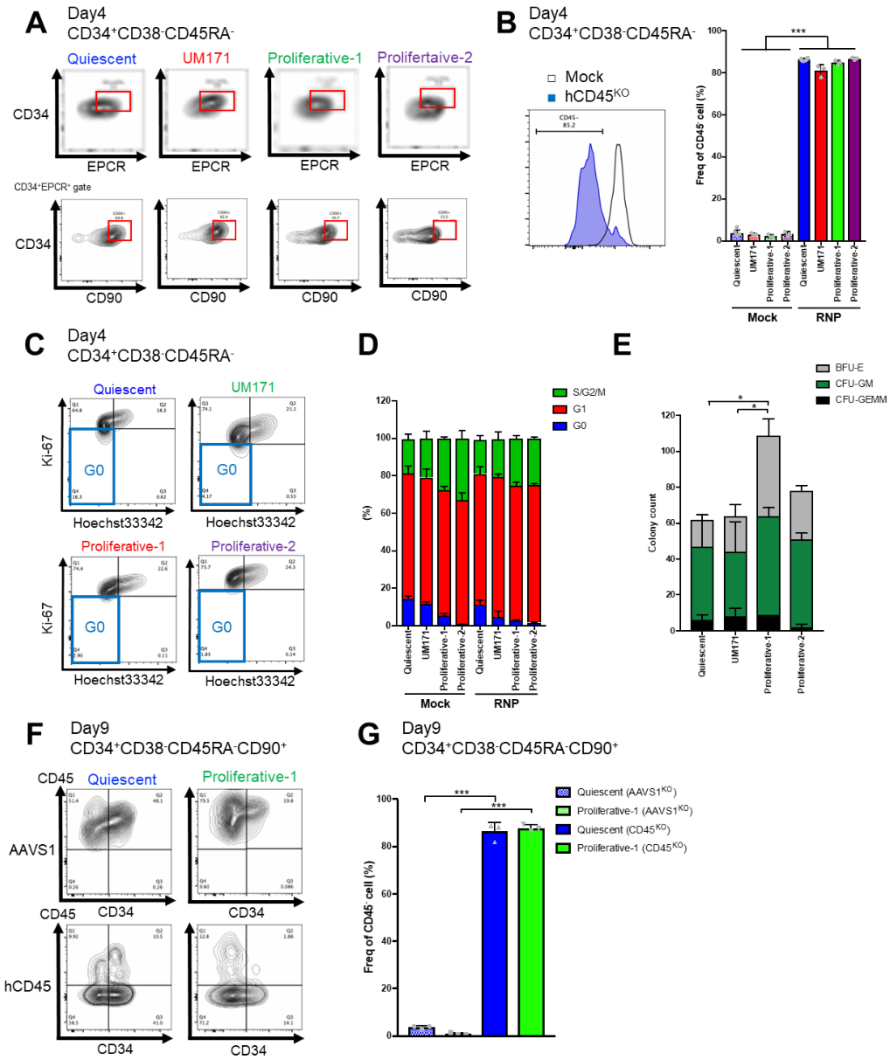


**Figure S7. Quiescent culture reverts human HSPCs to quiescence and maintains their primitive state after NHEJ-based editing, related to Figure 7**

(A) Representative flow cytometry plots of edited human HSPCs at 2 days after electroporation under the quiescence-maintaining condition, UM171-based condition, proliferative condition-1, and proliferative condition-2.

(B) Representative histogram of Cas9/CD45-sgRNA (blue). Mock cells were used as a negative control.

(C) Representative flow cytometry plots of cell cycle analysis of edited HSPCs at 2 days after electroporation under the quiescence-maintaining condition, UM171-based condition, proliferative condition-1, and proliferative condition-2 (mean ± SD, n = 3 per group).

(D) Cell cycle status at 2 days after electroporation in mock cells and cells electroporated with RNP.

(E) Number of colonies formed by genome-edited $CD34^{+}CD38^{-}CD45RA^{-}CD90^{+}$ cells (mean ± SD, n = 3 per group). The Tukey-Kramer multiple comparisons test was used.

(F) Representative flow cytometry plots of edited HSPCs at 7 days after electroporation under the quiescence-maintaining condition and proliferative condition-1.

(G) Frequency of $CD45^{-}$ cells at 7 days after electroporation under the quiescence-maintaining condition and proliferative condition-1. (mean ± SD, n = 3 from independent cell cultures). The Tukey-Kramer multiple comparisons test was used.